

LETTER

## Homogenization of periodic structures: One layer is “bulk”

To cite this article: A. N. M. Shahriyar Hossain *et al* 2022 *EPL* **138** 35001

View the [article online](#) for updates and enhancements.

You may also like

- [The influence of nonlinear scattering light distributions on the optical limiting properties of carbon nanotubes](#)  
Yaobing Xiong, Jinhai Si, Lihe Yan et al.
- [Nanofiber quantum photonics](#)  
Kali P Nayak, Mark Sadgrove,  
Ramachandrarao Yalla et al.
- [Quenched dynamics of two-dimensional solitary waves and vortices in the Gross–Pitaevskii equation](#)  
Qian-Yong Chen, P G Kevrekidis and  
Boris A Malomed

# Homogenization of periodic structures: One layer is “bulk”

A. N. M. SHAHRIYAR HOSSAIN<sup>1,2</sup>, IGOR TSUKERMAN<sup>1(a)</sup> and VADIM A. MARKEL<sup>3</sup>

<sup>1</sup> Department of Electrical and Computer Engineering, The University of Akron - OH 44325-3904, USA

<sup>2</sup> Department of Electrical, Computer, and Systems Engineering, Case Western Reserve University Cleveland, OH, USA 44106

<sup>3</sup> Departments of Radiology and Bioengineering and the Graduate Group in Applied Mathematics and Computational Science, University of Pennsylvania - Philadelphia, PA 19104, USA

received 7 September 2021; accepted in final form 18 February 2022  
published online 24 May 2022

**Abstract** – In homogenization theories of periodic electromagnetic structures, such as photonic crystals or metamaterials, it is commonly assumed that the accuracy of the effective medium representation is affected by the thickness of the sample in two different ways. The first factor is the optical length (OL) of wave propagation within the sample. For a large OL, minor deviations in the wave number may strongly affect transmission and reflection. The second factor is the putative convergence to bulk characteristics (CB), once the number of layers in the sample has approached or passed a certain threshold. The theoretical analysis and numerical examples of this letter show that, while the OL influence is real, CB is not actually relevant; in a sense, one layer is already “bulk”.



Copyright © 2022 EPLA

**Introduction.** – In existing effective medium theories of periodic electromagnetic structures, such as photonic crystals or metamaterials, it is commonly assumed that bulk behavior emerges only if the number of layers in a given structure is sufficiently large. For example, in [1] the effective medium representation of a certain family of hyperbolic metamaterials was determined to be accurate, typically, for five or more layers in the sample, although the results do vary depending on the composition of the structure. In [2], the authors studied particular metamaterial absorbers and found that four layers could already be accurately characterized as an effective medium. In other publications, as little as three layers were deemed sufficient [3,4]. Theoretical analysis of convergence to bulk behavior has in general been perceived as quite involved due to the complex behavior of surface waves [5,6].

The thickness of the sample is commonly believed to affect the accuracy of homogenization in two different ways. The first factor is the optical length (OL), defined as the phase shift of the wave propagating across the sample (a Bloch wave in a periodic structure or a plane wave in a homogeneous medium). For a large OL, minor deviations in the wave number may strongly affect the predicted transmission coefficient (especially its phase) as well as reflection. The second factor, as noted above, is the

putative convergence to bulk characteristics (CB), once the thickness of the sample (the number of layers) has approached or crossed a certain threshold.

While the OL influence is real, this letter shows, through theoretical analysis and numerical examples, that CB is a non-issue; in a sense, one layer is already bulk.

**Preliminaries.** – As in [5,7,8], we consider homogenization of periodic heterostructures characterized by the intrinsic scalar permittivity  $\tilde{\epsilon}(\mathbf{r})$ . The tilde sign is used for all lattice-periodic quantities. The individual constituents of the structure are assumed to be linear, local and intrinsically non-magnetic. The effective parameters, to be defined, are denoted by  $\epsilon_{\text{eff}}$  and  $\mu_{\text{eff}}$  and are in general second-rank tensors different from unity. We will also include into consideration the effective parameters of magnetoelectric coupling  $\chi_{\text{eff}}$  and  $\zeta_{\text{eff}}$ . The complete effective material tensor  $\mathcal{M}$  is represented by a matrix

$$\mathcal{M} \equiv \begin{pmatrix} \epsilon_{\text{eff}} & \chi_{\text{eff}} \\ \zeta_{\text{eff}} & \mu_{\text{eff}} \end{pmatrix}. \quad (1)$$

The dimension of  $\mathcal{M}$  is in general  $6 \times 6$  but can be reduced in special cases, such as 2D problems of  $s$  or  $p$  polarization.

Bloch-periodic functions (Bloch waves) are written in the following generic form:

$$f(\mathbf{r}) = \tilde{f}(\mathbf{r}) \exp(i\mathbf{q} \cdot \mathbf{r}), \quad (2)$$

<sup>(a)</sup>E-mail: igor@uakron.edu (corresponding author)

where  $\mathbf{q}$  is the Bloch wave vector. In the case of orthorhombic lattices, the lattice periodicity is expressed as

$$\tilde{f}(x + a_x, y + a_y, z + a_z) = \tilde{f}(x, y, z), \quad (3)$$

where  $a_x$ ,  $a_y$  and  $a_z$  are the lattice periods, and all points are simultaneously located within the heterostructure.

In the literature, Bloch waves (2) are sometimes interpreted as a result of coherent multiple scattering from the periodic lattice sites [9,10]. This interpretation can provide some physical insight, especially for 1D systems, and is fully consistent with the mathematical expression (2). The latter is standard and convenient for the analysis of this letter.

Fine-level fields—that is, the exact solutions to the macroscopic Maxwell equations—are denoted by small letters  $\mathbf{e}$ ,  $\mathbf{d}$ ,  $\mathbf{h}$  and  $\mathbf{b}$ . These fields should not be confused with the fields of atomic-scale electrodynamics; rather, they are assumed to be subject to the following constitutive relations:

$$\mathbf{d}(\mathbf{r}) = \tilde{\epsilon}(\mathbf{r}) \mathbf{e}(\mathbf{r}), \quad \mathbf{b}(\mathbf{r}) = \mathbf{h}(\mathbf{r}). \quad (4)$$

We adopt the  $\exp(-i\omega t)$  phasor convention at a given frequency  $\omega$ . The free-space wave number and wavelength are

$$k_0 = \omega/c; \quad \lambda = 2\pi/k_0. \quad (5)$$

**One layer is “bulk”.**— Consider a slab with  $N$  layers, thickness  $d = Na$  in the normal ( $n$ ) direction and infinite in the tangential directions  $\tau, z$ ,  $(n, \tau, z)$  being a right-handed system. The slab is illuminated by a plane wave propagating from the air ( $n < 0$ ) in the positive  $n$ -direction. The slab/air interface is at  $n = 0$ .

For algebraic simplicity, let us assume translational invariance in the  $z$ -direction and the  $s$  mode—one-component electric field  $\mathbf{e}(\mathbf{r}) = \hat{z} e(\mathbf{r})$  and the respective two-component magnetic field  $\mathbf{h}(\mathbf{r}) = \hat{n} h_n(\mathbf{r}) + \hat{\tau} h_\tau(\mathbf{r})$ , where  $\mathbf{r} \equiv (n, \tau)$ . The analysis is extendable to the general 3D case.

For a given  $q_\tau$ , consider a superposition of the forward and backward Bloch waves:

$$e(\mathbf{r}) = [c_1 \tilde{e}_1(n, \tau) \exp(iq_{n1}n) + c_2 \tilde{e}_2(n, \tau) \exp(iq_{n2}n)] \exp(iq_\tau \tau), \quad (6a)$$

$$h_\tau(\mathbf{r}) = [c_1 \tilde{h}_{\tau 1}(n, \tau) \exp(iq_{n1}n) + c_2 \tilde{h}_{\tau 2}(n, \tau) \exp(iq_{n2}n)] \exp(iq_\tau \tau), \quad (6b)$$

where  $c_{1,2}$  are undetermined coefficients and  $q_{n1} = -q_{n2}$  are the normal components of the respective Bloch wave vectors.

Let  $\mathbf{s}(n, \tau)$  be any vector field of the form

$$\mathbf{s}(n, \tau) = \tilde{\mathbf{s}}(n) \exp(ik_\tau \tau) \quad (7)$$

over any lattice cell face  $\mathbb{F}$  parallel to the  $\tau z$  plane. We will need the following operator, averaging the tangential

component of  $\mathbf{s}$  on  $\mathbb{F}$ :

$$\begin{aligned} \mathcal{A} \mathbf{s}(n) &\equiv a^{-2} \int_{\mathbb{F}} \mathbf{n} \times \mathbf{s}(n, \tau) \exp(-ik_\tau \tau) d\mathbb{F} \\ &= a^{-2} \int_{\mathbb{F}} \mathbf{n} \times \tilde{\mathbf{s}}(n, \tau) d\mathbb{F}, \end{aligned} \quad (8)$$

where the coordinate  $n$  corresponds to the location of  $\mathbb{F}$  and  $\mathbf{n}$  is the unit normal vector in the positive  $n$ -direction. Although the  $\mathcal{A}$  operator depends on  $\mathbb{F}$  and hence on  $n$ , with a slight abuse of notation we write  $\mathcal{A} \mathbf{s}(n)$  instead of  $\mathcal{A}(n) \mathbf{s}(n)$ .

Consider now an arbitrary lattice cell—for convenience,  $0 \leq n, \tau \leq a$ , although the relations below will apply to any cell. The amplitudes  $c_{1,2}$  of (6a), (6b) are linearly related to the averages of  $(e, h_\tau)$  on the left boundary of the cell,

$$\begin{bmatrix} c_1 \\ c_2 \end{bmatrix} = Z(0)^{-1} \begin{bmatrix} \mathcal{A} e(0) \\ \mathcal{A} h_\tau(0) \end{bmatrix}, \quad (9a)$$

$$Z(0) \stackrel{\text{def}}{=} \begin{bmatrix} \mathcal{A} e_1(0) & \mathcal{A} e_2(0) \\ \mathcal{A} h_{\tau 1}(0) & \mathcal{A} h_{\tau 2}(0) \end{bmatrix}. \quad (9b)$$

Since Bloch waves are defined up to an arbitrary factor, it is convenient to rescale the second row of  $Z(0)$  to unity and redefine  $Z(0)$  as

$$Z(0) = \begin{bmatrix} z_1 & z_2 \\ 1 & 1 \end{bmatrix}, \quad (10)$$

where  $z_1, z_2$  are Bloch impedances whose definition is clear from the context and is consistent with the one in [11,12].

Keeping this in mind, we can proceed with the standard transfer matrix analysis [13], except that Bloch waves rather than plane waves are involved. The total face-averaged field at the boundary  $n = a$  is

$$\begin{aligned} \begin{bmatrix} \mathcal{A} e(a) \\ \mathcal{A} h_\tau(a) \end{bmatrix} &= \begin{bmatrix} \mathcal{A} e_1(a) & \mathcal{A} e_2(a) \\ \mathcal{A} h_{\tau 1}(a) & \mathcal{A} h_{\tau 2}(a) \end{bmatrix} \begin{bmatrix} c_1 \\ c_2 \end{bmatrix} \\ &= \begin{bmatrix} \mathcal{A} e_1(0) & \mathcal{A} e_2(0) \\ \mathcal{A} h_{\tau 1}(0) & \mathcal{A} h_{\tau 2}(0) \end{bmatrix} Q \begin{bmatrix} c_1 \\ c_2 \end{bmatrix} \\ &\stackrel{(9a)}{=} Z(0) Q Z(0)^{-1} \begin{bmatrix} \mathcal{A} e(0) \\ \mathcal{A} h_\tau(0) \end{bmatrix} \equiv T_{\mathbb{C}} \begin{bmatrix} \mathcal{A} e(0) \\ \mathcal{A} h_\tau(0) \end{bmatrix}, \end{aligned} \quad (11)$$

where

$$Q = \begin{bmatrix} \exp(iq_{n1}a) & 0 \\ 0 & \exp(iq_{n2}a) \end{bmatrix}, \quad (12)$$

$$T_{\mathbb{C}} = Z(0) Q Z(0)^{-1}. \quad (13)$$

For an  $N$ -layer slab, let us define

$$T_N \stackrel{\text{def}}{=} T_{\mathbb{C}}^{-N} = Z(0) Q^{-N} Z(0)^{-1}. \quad (14)$$

Then the input-output relation for the slab is

$$\begin{bmatrix} E(0) \\ H_\tau(0) \end{bmatrix} = T_N \begin{bmatrix} E(Na) \\ H_\tau(Na) \end{bmatrix}, \quad (15)$$

where

$$E(0) \stackrel{\text{def}}{=} \mathcal{A}e(0), \quad E(Na) \stackrel{\text{def}}{=} \mathcal{A}e(Na), \quad (16a)$$

$$H_\tau(0) \stackrel{\text{def}}{=} \mathcal{A}h_\tau(0), \quad H_\tau(Na) \stackrel{\text{def}}{=} \mathcal{A}h_\tau(Na). \quad (16b)$$

Expressing  $E(Na)$ ,  $H_\tau(Na)$  via the amplitude of the transmitted field  $E_t$ , we have

$$\begin{bmatrix} E(0) \\ H_\tau(0) \end{bmatrix} = T_N \Psi_{\text{out}} E_t, \quad \Psi_{\text{out}} \stackrel{\text{def}}{=} \begin{bmatrix} 1 \\ z_{\text{out}}^{-1} \cos \theta_{\text{out}} \end{bmatrix}, \quad (17)$$

where  $z_{\text{out}}$  is the intrinsic impedance of the medium on the transmission side. Finally, writing  $E(0)$ ,  $H_\tau(0)$  in terms of the amplitudes of the incident and reflected waves  $E_i$ ,  $E_r$ , one obtains

$$\begin{bmatrix} E_i \\ E_r \end{bmatrix} = \Psi_{\text{in}}^{-1} T_N \Psi_{\text{out}} E_t, \quad (18a)$$

$$\Psi_{\text{in}} \stackrel{\text{def}}{=} \begin{bmatrix} 1 & 1 \\ z_{\text{in}}^{-1} \cos \theta_{\text{in}} & -z_{\text{in}}^{-1} \cos \theta_{\text{in}} \end{bmatrix}, \quad (18b)$$

where  $z_{\text{in}}$  is the intrinsic impedance of the medium on the side of incidence.

Although the algebra above may look cumbersome at first glance, we reiterate that it represents the standard layer-by-layer transfer matrix method applied to Bloch wave averages.

Due to (16), the differences between  $E$  and  $e$ , and between  $H$  and  $h$  on both sides of the slab (physically, these differences represent surface waves [5,6]) do not contain the zero-order harmonic with respect to  $\tau$  and hence do not affect the far fields, as long as  $a < \lambda_{\text{out}}$ . This brings us to the following key proposition.

**Proposition 1.** *At any given angle of incidence, reflection and transmission coefficients are identical for any structures with the same values of the Bloch wave numbers and impedances, regardless of the number of layers.*

Indeed, since matrices  $Z(0)$  and  $Q$  depend only on the Bloch parameters, the same is true for the cell transfer matrix  $T_C$  (13) and hence for the relationship between the incident/reflected/transmitted fields (18a).

Furthermore, Proposition 1, along with (18b), leads to a natural definition of homogenization. Since effective material parameters must be intrinsic to the structure and independent of the outside media, and since the only such intrinsic term in (18a) is the transfer matrix  $T_N$  (14), the goal of homogenization must be to approximate this matrix as accurately as possible with an analogous matrix corresponding to a hypothetical homogeneous medium; that is, to minimize, with respect to a desired norm, the matrix difference

$$\Delta T \stackrel{\text{def}}{=} T_N - T_{Nh} = Z(0) Q^{-N} Z(0)^{-1} - Z_h(0) Q_h^{-N} Z_h(0)^{-1}, \quad (19)$$

where the subscript “ $h$ ” indicates the respective matrix for a homogeneous layer with given parameters.

$T_N$  involves four variables —the Bloch impedances  $z_1$ ,  $z_2$  and wave numbers  $q_{n1}$ ,  $q_{n2}$ — which are functions of the angle of incidence. If the effective parameters are also allowed to depend on the angle, as done in some existing theories (e.g., [14,15]), then matrices  $Z_h(0)$ ,  $Q_h$  may be angle-dependent as well. Under these assumptions, perfect homogenization is possible, since the material tensor has 9 adjustable entries, allowing an ideal fit for the four parameters of  $T_N$ . Hence we arrive at the following known result.

**Proposition 2.** *If the effective parameters are allowed to depend on the angle of incidence, then homogenization can be perfect irrespective of the number of layers.*

On the other hand, for an effective tensor independent of illumination conditions [7,16], error  $\Delta T$  (19) is in general non-zero. For small deviations  $\delta z_{1,2} = z_{1,2h} - z_{1,2}$ ,  $\delta q_{1,2} = q_{1,2h} - q_{1,2}$ , perturbation analysis gives the Frobenius norm

$$\|\Delta T\|_F = \mathcal{O}(\delta z_{1,2}, N \delta q_{1,2}). \quad (20)$$

The  $N$  factor is a clear manifestation of the OL effect. At the same time, there is no indication of the putative CB phenomenon.

While the  $s$  mode was considered to fix ideas, the analysis and results can be extended to arbitrary structures with arbitrary excitation, even for polarization rotation. The only stipulation in this general case is existence, for a given angle of incidence, of four linearly independent Bloch waves<sup>1</sup> (backward/forward, with two different polarizations). The  $Z$ ,  $T_C$  and  $T_N$  matrices are in general  $4 \times 4$  and act on the 4-vectors  $(E_{\tau 1}, E_{\tau 2}, H_{\tau 1}, H_{\tau 2})$ .

### Numerical examples. –

*Layered media.* Under plane wave illumination, fields in periodic layered media (with a finite thickness  $d = Na$  in the normal  $n$ -direction, and infinite in the  $\tau z$  directions) are mathematically described by ordinary differential equations with respect to  $n$  and therefore are linear combinations of two linearly independent solutions, which can conveniently be chosen as Bloch waves. Consequently, there are no surface waves (“transition layers”), and it follows from the analysis above that the retrieved effective material parameters must be completely independent of the number of layers.

As a numerical example, we consider a benchmark problem established in previous publications [7,8,16], fig. 1. The lattice cell has mirror symmetry and contains three dielectric layers  $(a, b, a)$ , with their respective permittivities  $\epsilon_a, \epsilon_b, \epsilon_a$  and widths  $(1/4, 1/2, 1/4) a$ . The materials are intrinsically non-magnetic. Free space is assumed on the sides of illumination and transmission;  $s$ -polarization is considered ( $E = E_z$ ,  $\mathbf{H}$  is in the  $n\tau$  plane, with different directions and magnitudes for the incident, reflected and transmitted waves).

For a numerical investigation, we have adopted straight-forward parameter retrieval, to avoid any real or perceived

<sup>1</sup>Linear independence is stipulated here only for the *boundary values* of the respective Bloch waves.

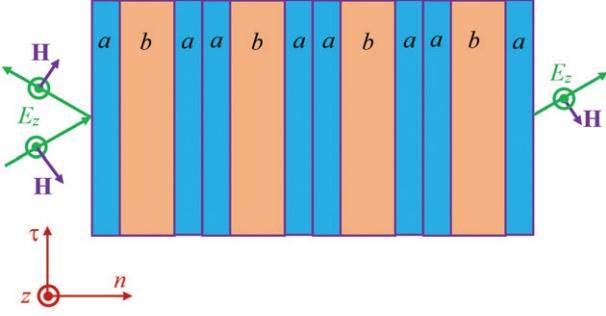


Fig. 1: The setup for the example of a layered structure. The lattice cell contains three layers,  $aba$ , with their respective widths  $w_a, w_b, w_a$  and dielectric permittivities  $\epsilon_a, \epsilon_b, \epsilon_a$ . Oblique incidence,  $s$ -polarization ( $E = E_z, \mathbf{H}$  in the  $n\tau$  plane).

idiosyncrasies of any other homogenization procedures. Finding the material tensor from the transmission and reflection data at normal incidence only is well known to be an underdetermined problem [16,17]. This is related mathematically to the multivaluedness of the inverse trigonometric functions, and physically to a varying number of wavelengths within a homogenized slab with a high undetermined optical density. Retrieval becomes well posed if, in addition to normal incidence, other angles are taken into account. A semi-analytical procedure for parameter retrieval at angles *around* normal incidence is detailed in [16].

As a simple alternative, here we apply numerical optimization for the following set of angles of incidence:

$$\underline{\theta} = \{0, \pm 5^\circ, \pm 10^\circ, \pm 45^\circ\}. \quad (21)$$

The objective function is

$$G(\mathcal{M}, \underline{\theta}, N) = \|\underline{R}_h - \underline{R}_{\text{layered}}\|_2 + \|\underline{T}_h - \underline{T}_{\text{layered}}\|_2. \quad (22)$$

Here  $\underline{R}_h, \underline{R}_{\text{layered}}, \underline{T}_h, \underline{T}_{\text{layered}}$  are the Euclidean vectors of the complex reflection and transmission coefficients, respectively, corresponding to a given set of incidence angles  $\underline{\theta}$ ; subscripts “ $h$ ” and “layered” correspond to the homogenized slab with a material tensor  $\mathcal{M}$  and to the actual layered structure, respectively. Similar notation is used for the sets of transmission coefficients. Minimization of the functional  $G$  (22) was performed numerically using Matlab’s built-in function `fminsearch`, with the tolerance of  $10^{-6}$ . The number of layers  $N$  varied from 1 through 10. For  $a/\lambda = 0.2$  (*i.e.*, the vacuum wavelength equal to five cell sizes), and for  $\epsilon_a = 4 + 0.1i, \epsilon_b = 1$  the effective parameters are found to be  $\epsilon_{\text{eff}} = 2.0397 + 0.0165i, \mu_{nn,\text{eff}} = 1.2347 + 0.0826i, \mu_{\tau\tau,\text{eff}} = 1.2883 + 0.0163i$ . These results are entirely independent of the number of layers.

*A 3D plasmonic structure.* Our second example is more involved: a rectangular silver parallelepiped  $d_n \times d_\tau \times d_z$  at the center of an otherwise empty lattice cell  $a \times a \times a$  (fig. 2). Illumination is by an  $s$ -polarized plane wave. Due to symmetry, the effective material tensor is

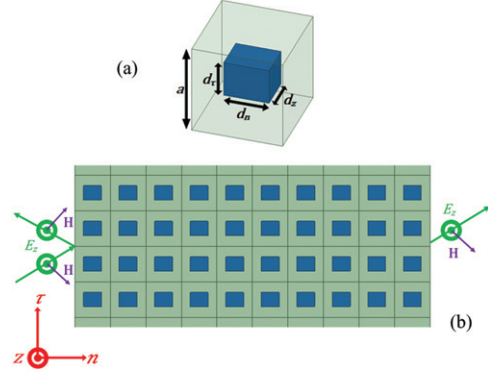


Fig. 2: (a) The unit cell for the 3D example: a rectangular silver cuboid ( $d_n \times d_\tau \times d_z$ ) in a host material with the permittivity 1.0;  $d_n = 100$  nm,  $d_\tau = d_z = 80$  nm. The cell size is  $a_x = a_y = a_z = a = 200$  nm. (b) Top view of the sample structure (truncated in the  $\pm\tau$ -direction); illumination by an  $s$ -polarized plane wave from the left. Periodicity in the  $z$ -direction.

diagonal. Particular geometric parameters chosen for this example are  $d_n = 100$  nm,  $d_\tau = d_z = 80$  nm,  $a = 200$  nm.

We use the following form of the Drude model for silver:

$$\epsilon(\lambda) = \epsilon_0 - \frac{1}{\lambda_p^2/\lambda^2 + i\tilde{\gamma}\lambda_p/\lambda}, \quad (23)$$

where  $\lambda = 2\pi c/\omega$  is the free-space wavelength corresponding to a given frequency  $\omega$ ;  $\epsilon_0 = 5$ ;  $\tilde{\gamma} = 1/526.3$ ;  $\lambda_p = 136.1$  nm [18].

For our full-wave 3D simulations, we have chosen the publicly available Rigorous Coupled Wave Analysis (RCWA) [19,20] tool  $S^4$  [21], which has been extensively used and tested by various research groups and in our prior publications [22,23].  $S^4$  is freely available on the nanohub server [24].

RCWA splits up a 3D structure with 2D periodicity into thin slices. 2D Fourier expansions within each slice are matched across the interface boundaries between the slices to enforce the continuity of the tangential field components. In most our simulations, the number of in-plane Fourier coefficients is  $N_s = 100$ , but we have also verified consistency of the results in selected cases with  $N_s = 400$ . Transmission and reflection coefficients have been computed for structures with one to ten layers at the free-space wavelength  $\lambda = 1200$  nm.

The parameter retrieval procedure and the objective function (22) are the same as in the previous example.

Plotted in figs. 3–5 are the real parts of the retrieved effective parameters  $\epsilon_{\text{eff}}, \mu_{n,\text{eff}}$  and  $\mu_{\tau,\text{eff}}$  for the 3D plasmonic heterostructure as a function of the number of layers. (The imaginary parts of these parameters are of the order of 0.01 and not shown). All parameters exhibit just minor deviations from a constant value, and, consistent with our analysis above, there is no evidence of a gradual transition to bulk values.

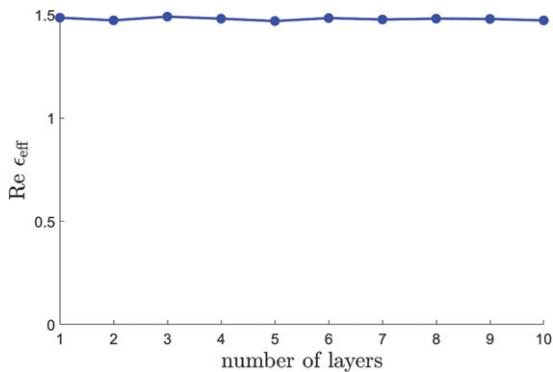


Fig. 3: The real part of the retrieved  $\epsilon_{\text{eff}}$  for the 3D plasmonic heterostructure *vs.* the number of layers.  $\lambda = 1200$  nm,  $a = 200$  nm, angles used for retrieval (deg.): 0, 5, 10, 45. There is no indication of gradual “convergence to bulk”.

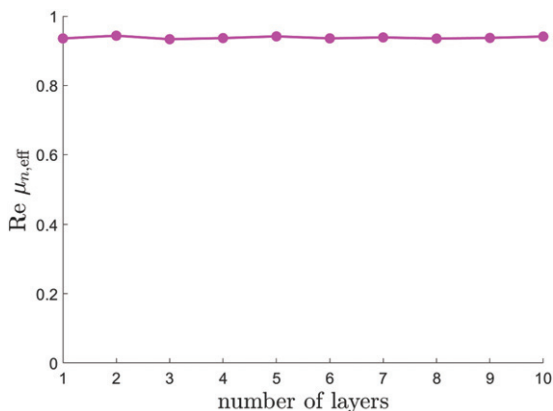


Fig. 4: Same as fig. 3 but for  $\mu_{n,\text{eff}}$ .

This conclusion can be reinforced by looking at the results in a slightly different way. Suppose that parameter retrieval is performed just for a single layer of the structure under consideration. By conventional wisdom, these parameters would not be applicable to the “bulk”. However, the numerical results paint a different picture—in accord with the theory presented on page 2 of this letter. Compared in fig. 6 are the absolute values of the reflection coefficients for the actual heterostructure and the respective homogenized slab, as functions of the number of layers, for  $\theta_{\text{inc}} = 45^\circ$ . The agreement between the two is evident for all numbers of layers, despite the fact that parameter retrieval was performed for a single layer only. (Numerical results for other angles of incidence lead to the same conclusion.) A similar agreement is manifest for the phase angle of  $R$  (fig. 7) as well as for the magnitudes and phases of the transmission coefficients (figs. 8, 9).

There is, however, an important caveat. In the case under consideration, effective parameters are virtually independent of the angle of incidence. This means that the heterostructure is homogenizable in the traditional sense. Then, as our theory and results show, effective parameters

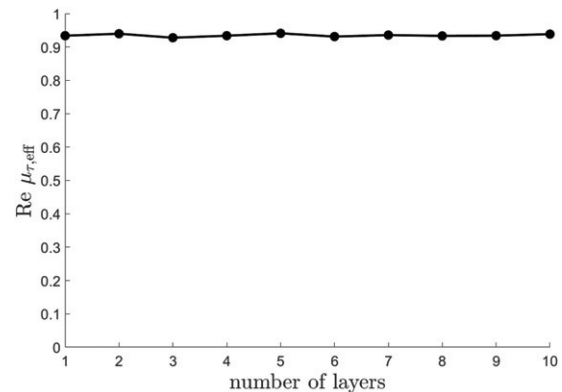


Fig. 5: Same as fig. 3 but for  $\mu_{\tau,\text{eff}}$ .

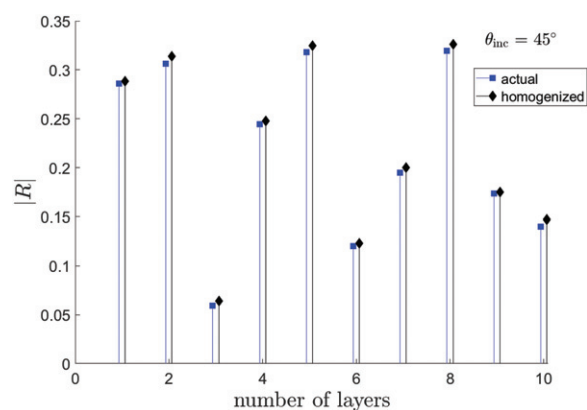


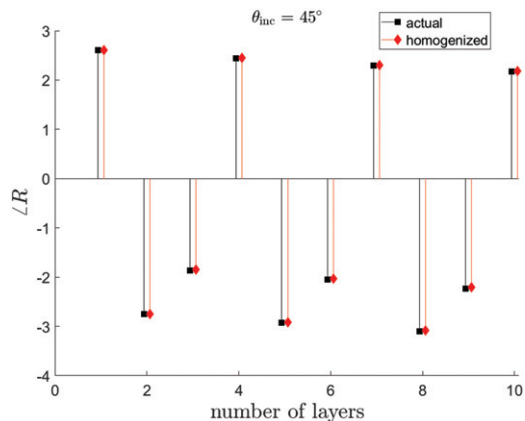
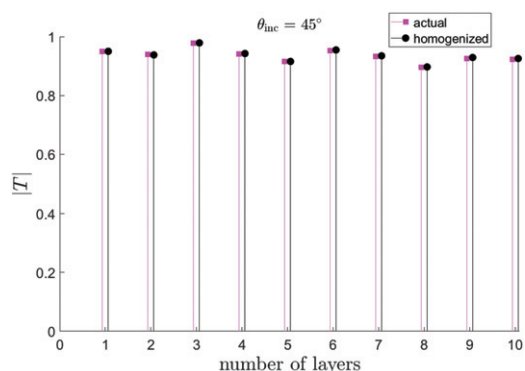
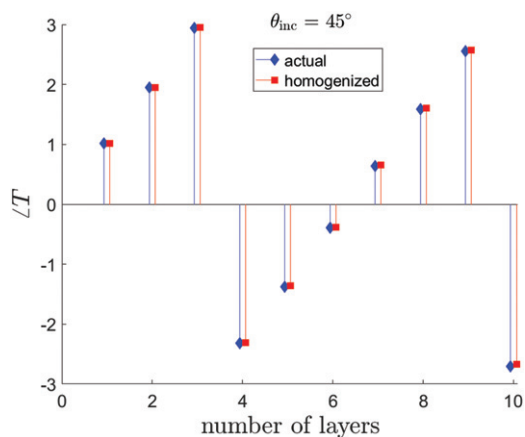
Fig. 6: The absolute value of the reflection coefficient  $R$  *vs.* the number of layers, for the actual heterostructure and the respective homogenized slab.  $\lambda = 1200$  nm; the angle of incidence is  $45^\circ$  (numerical results for other angles lead to the same conclusions). The stems are displaced slightly relative to their integer positions for visual clarity.

do not depend on the number of layers. On the other hand, if parameters are allowed to be illumination dependent<sup>2</sup>, then homogenization can render reflection and transmission coefficients perfectly, and the effective (angle-dependent) parameters are, yet again, independent of the number of layers.

As noted in the introduction, parameters retrieved for a small number of layers were often recognized by various research groups to be physically meaningful [1–4]; this is consistent with the primary message of this letter. If a dependence of effective parameters on the number of layers is observed, it is likely due to a combination of factors: i) numerical and/or measurement errors and fabrication tolerances, and ii) structure not being homogenizable because of its complexity and/or wavelengths being short.

**Discussion and conclusion.** — Homogenization is aimed at replacing a periodic heterostructure with a

<sup>2</sup> Here we do not debate the usefulness of illumination-dependent parameters; this was done in [16].

Fig. 7: Same as in fig. 6, but for the phase angle of  $R$ .Fig. 8: Same as in fig. 6, but for  $|T|$ .Fig. 9: Same as in fig. 7, but for the phase angle of  $T$ .

homogeneous sample of the same size and shape, in such a way that transmission and reflection (or, more generally, scattering) of the incident radiation remains unchanged or changes as little as possible. In the case of a homogeneous slab illuminated by a linearly polarized plane wave at any fixed angle of incidence, the field within the slab, under rather general assumptions, is a superposition of two independent plane waves – forward and backward. Notably, the same is true for the periodic structure, except

that the superposition is of the forward and backward *Bloch waves* rather than plane waves.

This leads to the following correspondence principle, stated as Proposition 1 in this letter. If the boundary impedance and wave number for a homogeneous layer are the same as those of the periodic structure, the scattering parameters in these two cases are indistinguishable at any given angle of incidence, regardless of the number of layers. That is, the effective parameters corresponding to a single layer are the same as the bulk ones. This conclusion is supported by theoretical analysis and numerical simulations in the letter.

For simplicity, in the numerical examples of this letter we considered symmetric lattice cells. However, the analysis, results and conclusions do not depend on symmetry. Indeed, structures lacking mirror symmetry can be homogenized if magnetoelectric coupling is introduced [25]; the homogenization accuracy is then comparable with that of similar symmetric structures, and the effective material tensor is still independent of the number of layers—that is, one layer is still “bulk”.

One may wonder why the main point of this letter (one layer is already “bulk”) has not been noted previously. We surmise one general reason and a few incidental ones. Generally, homogenization of metamaterials is quite involved due to its non-asymptotic character [7]: to achieve unusual physical effects, the lattice cell size  $a$  cannot be vanishingly small relative to the vacuum wavelength  $\lambda$  [26]. The complex field behavior in large lattice cells ( $a \sim (0.2\text{--}0.4)\lambda$  in many cases of practical interest) tends to reduce the accuracy of homogenization; this is often interpreted as effects of spatial dispersion. Dependence of the effective parameters on the number of layers (or the absence of such dependence) is thereby obscured. The incidental reasons alluded to above depend on the nature of research. Experimental work is likely to be affected by measurement errors and fabrication tolerances [1]. In analytical and numerical studies [2–4], dependence of the effective parameters on the number of layers has not been the main thrust of investigations and has not been studied in detail.

Since the analysis of this letter relies in a principal way on periodicity and Bloch modes, the conclusions do not apply to random or pseudorandom structures, where considerations are qualitatively different.

\*\*\*

Research of ANMSH and IT was supported in part by the US National Science Foundation awards DMS-1216970 and DMS-1620112. The authors thank PETER BERMEL and ZE WANG (Purdue University) for their help with  $S^4$ /nanohub simulations.

*Data availability statement:* The data that support the findings of this study are available upon reasonable request from the authors.

*Note added in proofs:* The authors gratefully acknowledge helpful discussions with CARSTEN ROCKSTUHL in

the spring of 2022, after this letter was accepted. Several papers by the Rockstuhl group are closely related to the subject of this letter and will be addressed in our future work [27,28].

## REFERENCES

- [1] SUKHAM J., TAKAYAMA O., MAHMOODI M., SYCHEV S., BOGDANOV A., TAVASSOLI S. H., LAVRINENKO A. V. and MALUREANU R., *Nanoscale*, **11** (2019) 12582.
- [2] LU G., WU F., ZHENG M., CHEN C., ZHOU X., DIAO C., LIU F., DU G., XUE C., JIANG H. and CHEN H., *Opt. Express*, **27** (2019) 5326.
- [3] CHEN X., GRZEGORCZYK T. M., WU B.-I., PACHECO J. and KONG J. A., *Phys. Rev. E*, **70** (2004) 016608.
- [4] PORS A., TSUKERMAN I. and BOZHEVOLNYI S. I., *Phys. Rev. E*, **84** (2011) 016609.
- [5] MARKEL V. A. and SCHOTLAND J. C., *Phys. Rev. E*, **85** (2012) 066603.
- [6] XIONG X. Y., JIANG L. J., MARKEL V. A. and TSUKERMAN I., *Opt. Express*, **21** (2013) 10412.
- [7] TSUKERMAN I. and MARKEL V. A., *Proc. R. Soc. A*, **470** (2014) 20140245.
- [8] TSUKERMAN I., *Phys. Lett. A*, **381** (2017) 1635.
- [9] RAUTIAN S. G., *Opt. Spectrosc.*, **104** (2008) 112.
- [10] JOANNOPOULOS J. D., JOHNSON S. G., WINN J. N. and MEADE R. D., *Photonic Crystals: Molding the Flow of Light*, second edition (Princeton University Press, Princeton, NJ) 2008.
- [11] SIMOVSKI C. R., *Opt. Spectrosc.*, **107** (2009) 766.
- [12] SIMOVSKI C. R., *J. Opt.*, **13** (2011) 103001.
- [13] YE H. P., *Optical Waves in Layered Media* (John Wiley, Hoboken, NJ) 2005.
- [14] CHEBYKIN A. V., ORLOV A. A., SIMOVSKI C. R., KIVSHAR Y. S. and BELOV P. A., *Phys. Rev. B*, **86** (2012) 115420.
- [15] CHERN R.-L., *Opt. Express*, **21** (2013) 16514.
- [16] MARKEL V. A. and TSUKERMAN I., *Phys. Rev. B*, **88** (2013) 125131.
- [17] SMITH D., SCHULTZ S., MARKOŠ P. and SOUKOULIS C., *Phys. Rev. B*, **65** (2002) 195104.
- [18] RASSKAZOV I. L., KARPOV S. V. and MARKEL V. A., *J. Opt. Soc. Am. B*, **31** (2014) 2981.
- [19] MOHARAM M. G. and GAYLORD T. K., *J. Opt. Soc. Am.*, **71** (1981) 811.
- [20] MOHARAM M. G., POMMET D. A., GRANN E. B. and GAYLORD T. K., *J. Opt. Soc. Am. A*, **12** (1995) 1077.
- [21] LIU V. and FAN S., *Comput. Phys. Commun.*, **183** (2012) 2233.
- [22] HOSSAIN A. S. and TSUKERMAN I., *Phys. Lett. A*, **398** (2021) 127278.
- [23] HOSSAIN A., *Metamaterials: 3-D Homogenization and Dynamic Beam Steering*, Master’s Thesis, The University of Akron (2019).
- [24] KANG J., WANG X., BERMEL P. and LIU C., *S4: Stanford Stratified Structure Solver*, <https://nanohub.org/resources/s4sim>.
- [25] TSUKERMAN IGOR, SHAHRIYAR HOSSAIN A. N. M. and CHONG Y. D., *EPL*, **133** (2021) 17003.
- [26] TSUKERMAN I., *J. Opt. Soc. Am. B*, **25** (2008) 927.
- [27] ROCKSTUHL CARSTEN, PAUL THOMAS and LEDERER FALK, *Phys. Rev. B*, **77** (2008) 035126.
- [28] PAUL THOMAS, MENZEL CHRISTOPH, SMIGAJ WOJCIECH, ROCKSTUHL CARSTEN, LALANNE PHILIPPE and LEDERER FALK, *Phys. Rev. B*, **84** (2011) 115142 (see especially sect. III).